Vol. 539: 65–76, 2015
doi: 10.3354/meps11472

MARINE ECOLOGY PROGRESS SERIES
Mar Ecol Prog Ser

Published November 12

Patchiness and depth-keeping of copepods in response to simulated frontal flows

A. C. True[1,4], D. R. Webster[1,*], M. J. Weissburg[2], J. Yen[2], A. Genin[3]

[1]School of Civil and Environmental Engineering, Georgia Institute of Technology, Atlanta, Georgia 30332-0355, USA
[2]School of Biology, Georgia Institute of Technology, Atlanta, Georgia 30332-0230, USA
[3]Department of Ecology, Evolution & Behavior,
The Hebrew University of Jerusalem and The Interuniversity Institute for Marine Sciences of Eilat, PO Box 469, Eilat 88103, Israel
[4]*Present address:* Civil, Environmental, and Architectural Engineering, University of Colorado, Boulder, Colorado 80309-0428, USA

ABSTRACT: When presented with a fine-scale upwelling or downwelling shear flow in a laboratory flume, 2 tropical copepods from the Red Sea, *Acartia negligens* and *Clausocalanus furcatus*, performed a set of behaviors that resulted in apparent depth-keeping and the potential for producing patchiness. Analyses of free-swimming trajectories revealed a behavioral threshold shear deformation rate value of 0.05 s^{-1} for both species. This threshold marked the transition to a range of behaviorally relevant shear deformation rate values and triggered statistically significant changes in path kinematics (i.e. relative swimming speed and turn frequency) in the shear layer versus out-of-layer. Gross path characteristics (i.e. net-to-gross displacement ratio, NGDR, and proportional vicinity time, PVT) were also significantly different in the shear layer treatments compared to controls. The vertical net-to-gross displacement ratio (VNGDR) was introduced here to explain a spectrum of depth-keeping behaviors. The mean value of VNGDR significantly increased in the treatments and suggested that the upwelling and downwelling shear layers induced vertical transport with large net vertical displacement. However, histograms of VNGDR revealed a bimodality, which indicated that a sizable portion of the population was also displaying depth-keeping behavior (low VNGDR). Those copepod trajectories not displaying depth-keeping behavior at the scale of the observation (high VNGDR) predominately consisted of copepods attempting to swim against the flow, thereby resisting vertical advection, which is another potential depth-keeping mechanism. Preferential depth-keeping was consistent with *in situ* acoustic tracking studies and could improve survival by increasing residence time near fronts, which are often coincident with food and mates.

KEY WORDS: Mechanosensory cue · Depth-keeping · Patchiness · Shear flow · *Acartia negligens* · *Clausocalanus furcatus*

INTRODUCTION

Numerous studies have observed elevated abundances of zooplankton, including copepods, in the region surrounding fronts (e.g. Herman et al. 1981, Dubischar et al. 2002, Landry et al. 2012, Munk 2014), and these regions often had elevated primary and secondary production (Largier 1993, McClatchie et al. 2012). Elevated abundances have been attributed to copepods being attracted to fronts due to high availability of food (Largier 1993, Genin 2004), copepods spending more time foraging near fronts (McManus & Woodson 2012), or enhanced copepod population growth in these regions (Genin 2004). Further, species-specific distributions have been observed in and around fronts, suggesting that more than one explanation of elevated abundances is likely (Mann & Lazier 2006, Greer et al. 2015).

*Corresponding author: dwebster@ce.gatech.edu

Fronts generally consist of complex 3-dimensional flows that include upwelling and/or downwelling currents (Wolanski & Hamner 1988, Mann & Lazier 2006). They often span a relatively narrow horizontal extent and are characterized by large gradients in the horizontal direction (Mann & Lazier 2006). Biophysical coupling between animal behavior and local hydrodynamics produces complex population distributions at and near fronts (Franks 1992, McManus & Woodson 2012, Greer et al. 2015). For example, copepods form accumulations by swimming against upwelling currents at intermediate depths during daytime illumination and by swimming against downwelling currents in the upper photic layer (Genin 2004).

To accurately assess the full ecological implications of patchy productivity in frontal regions, it is critical to quantify the individual and interactive effects of various biological, chemical, and physical mechanisms at relevant spatio-temporal scales (e.g. Folt & Burns 1999, Lennert-Cody & Franks 1999). For example, via simulations, Franks (1992) found that swimming behavior and fluid velocity structure control the scales of patchiness. While these simulations were very informative for understanding copepod accumulations in and near fronts, McManus & Woodson (2012) noted that a largely unknown and crucial component is species-specific animal behavior. Further, it is becoming increasingly apparent that behavioral responses to small-scale characteristics of oceanic features, such as fronts, have the capacity to influence large-scale distributions of organisms, trophic interactions, and productivity (Woodson et al. 2014).

Hydrodynamic cues (i.e. deformation rate, rotation or vorticity, and acceleration) play a major role in copepod behavior. Primary examples include mediating predator–prey interactions (Fields & Yen 1997, Kiørboe & Visser 1999) and finding mates (Yen et al. 1998). Similarly, Woodson et al. (2005, 2007a,b) observed copepods responding to thin layers of velocity shear (flow aligned horizontally with vertical gradients) with increased swimming speed and turning frequency that resulted in an increased residence time near those layers. Hence, patchy distributions of copepods resulted from the animals' ability to detect and behaviorally respond to environmental flow structure at small scales. Although threshold deformation rates for escape response have been established for a variety of species (summarized by Woodson et al. 2014), threshold deformation rates for behavioral responses that underlie aggregation and how hydrodynamic information, including flow and gradient directionality, affects behavior remain poorly understood.

This study sought to understand how the calanoid copepods *Acartia negligens* and *Clausocalanus furcatus* respond behaviorally to upwelling and downwelling flow fronts (i.e. flow aligned in the vertical direction with horizontal gradients), and whether behavioral responses can explain observed depth maintenance and patchiness.

MATERIALS AND METHODS

Upwelling and downwelling flow treatments

A recirculating flume incorporating a laminar, planar free jet was designed to create horizontal gradients of vertical velocity that are consistent with oceanic flows, similar to that previously used to study horizontal thin layers (Woodson et al. 2005). The apparatus used here consisted of an elevated constant head tank (28 l) with a free surface overflow to ensure a time-invariant supply of potential energy to the flow system. The sealed test section (1 m × 30 cm × 30 cm) was constructed of clear acrylic for optical access and was aligned vertically (with the gravity vector) (Fig. 1). The test section could be inverted to create both upwelling and downwelling free shear flows. The flow passed through a specially designed slot jet nozzle (316 SS, jet opening 1 × 25 cm) to create a laminar planar jet (the Bickley jet) in the vertical direction. A needle valve and flowmeter maintained and quantified the volumetric flow rate. Note that the addition of the back pressure reservoir in the upwelling flow configuration greatly improved flow stability by preventing the formation of a siphon flow between the outlet of the flume and the secondary reservoir.

A volumetric flowrate of 0.06 $m^3\ h^{-1}$ was selected to produce a well defined and ecologically relevant laminar flow field with a jet exit velocity, U_j, of 6.7 mm s^{-1}. For comparison, Genin et al. (2005) reported upwelling and downwelling velocities in the range of 5.6 to 15 mm s^{-1} at 2 coastal sites in the northern Gulf of Aqaba, Red Sea. The jet Reynolds number, $Re_j = U_j d/\nu$, was 52, where $d = 1$ cm is the jet nozzle width and ν is the fluid kinematic viscosity. Thus, the flow was in the transitionally stable and laminar regime. The velocity field was quantified via particle image velocimetry (PIV) (Raffel et al. 1998); details of the hardware and image processing software are provided in Dasi et al. (2007). Fig. 2a shows the velocity and shear deformation (strain) rate fields

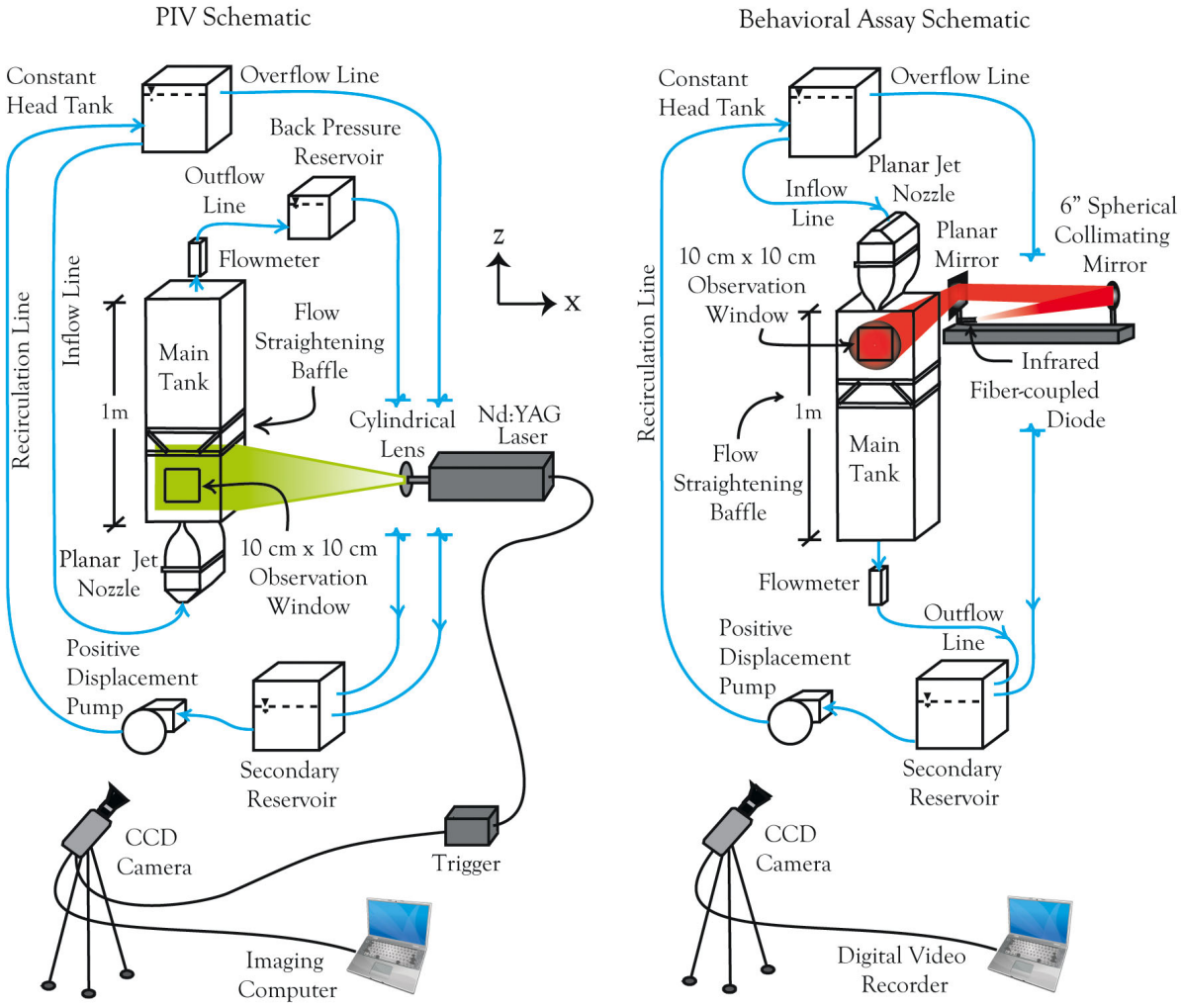

Fig. 1. Schematic of the apparatus for particle image velocimetry (PIV) flow characterization (left panel, arbitrarily in the upwelling configuration) and copepod behavioral assays (right panel, arbitrarily in the downwelling configuration)

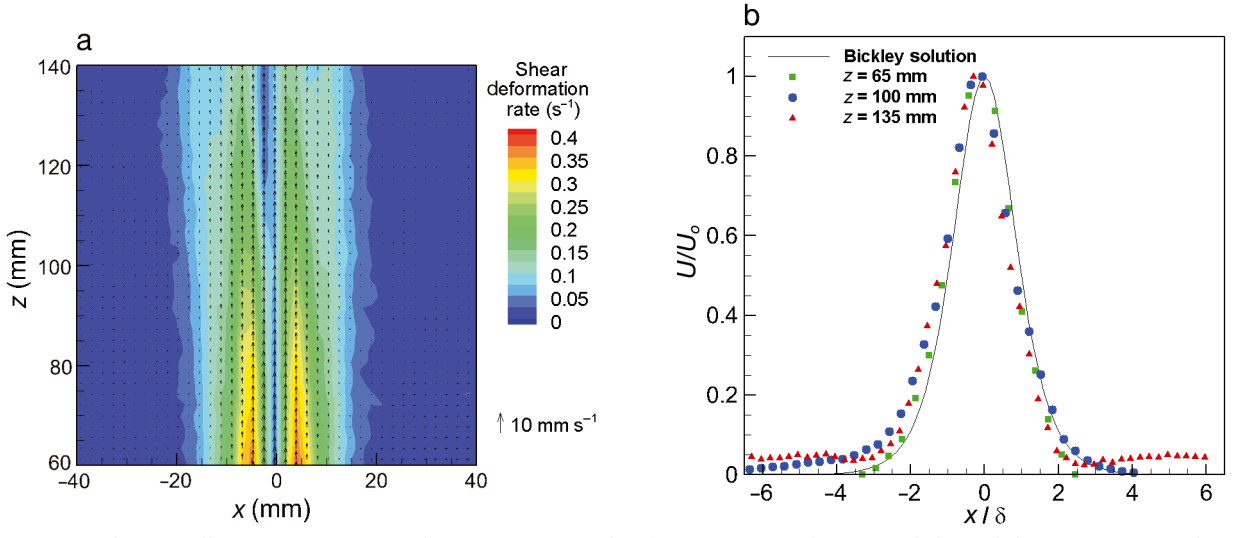

Fig. 2. For the upwelling treatment, (a) velocity (vectors, with reference vector shown) and shear deformation rate (color contours) fields, and (b) normalized velocity profiles. U_o is the centerline velocity, δ is the jet half-width, x is the lateral coordinate, and z is the vertical coordinate with the origin at the nozzle exit location

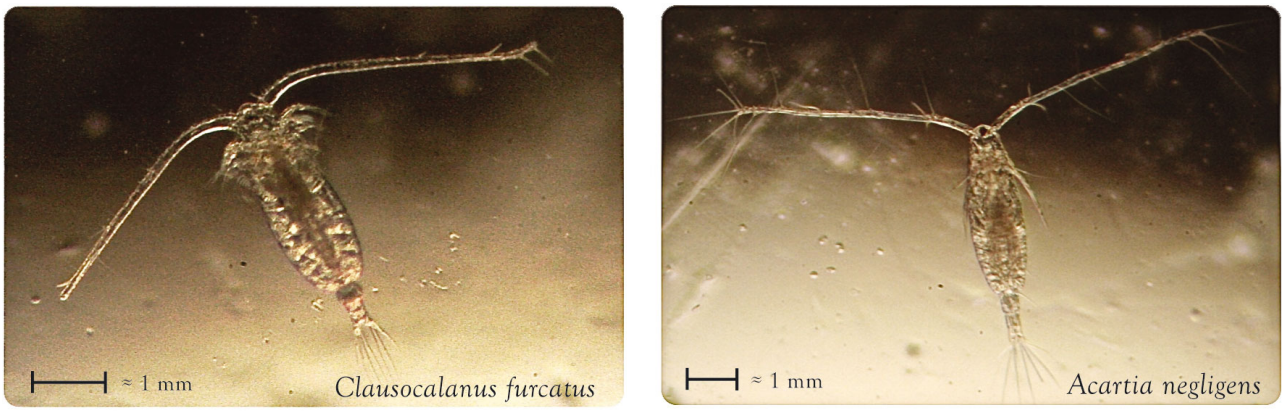

Fig. 3. The tropical copepods *Clausocalanus furcatus* (cruising swimmer) and *Acartia negligens* (hop-sink swimmer) collected on a fringing reef in the Red Sea, Eilat, Israel (photographs by Ellen True)

for the upwelling flow treatment. The field was nearly symmetric about $x = 0$, and the lateral velocity profiles were self-similar and closely matched the analytical Bickley jet solution (Fig. 2b; True 2011). The peak value in the transverse shear deformation rate profile varied from approximately 0.35 to 0.12 s^{-1} with distance downstream from the jet exit (i.e. between $z = 5$ cm and $z = 15$ cm). The downwelling flow field (not shown here) agreed very well with the upwelling field, with the obvious exception that the flow was in the opposite direction (True 2011).

Copepod behavioral assays

Two species with different swimming behaviors were selected (Fig. 3): *Acartia negligens*, which uses a hop-and-sink mode of swimming, and *Clausocalanus furcatus*, which exhibits active swimming with frequent changes of direction (Mazzocchi & Paffenhöfer 1999, Uttieri et al. 2008). *C. furcatus* was considered to be an herbivore (Prado-Por 1983, Mazzocchi & Paffenhöfer 1999), although later studies (Cornils et al. 2007b) have found that this species is a non-selective feeder that ingests abundant particles, including flagellates and ciliates. *C. furcatus* occurs in tropical and subtropical oceans, is one of the most abundant calanoids in oligotrophic waters (Peralba & Mazzocchi 2004), and its biology is relatively well described (Mazzocchi & Paffenhöfer 1998, 1999, Peralba & Mazzocchi 2004, Cornils et al. 2007b, Uttieri et al. 2008,). Much less is known about *A. negligens*, which is considered to be an herbivore (Prado-Por 1983).

Both species are common in the upper water column of the Gulf of Aqaba (Cornils et al. 2007a,b) where they were collected and where upwelling and downwelling currents are dominant features along the coasts. The prevailing northerly winds in the Gulf generate upwelling along the east coast and downwelling in the west (Labiosa et al. 2003). In addition, both small-scale (10's km) cyclonic and anticyclonic eddies occur along the Gulf (Manasrah et al. 2004). Therefore, encountering vertical currents at a range of spatial scales is likely to be common for both species. As far as the authors are aware, the relationship between these species and such hydrodynamic oceanic features has not yet been examined.

A. negligens and *C. furcatus* were collected off the dock of the Interuniversity Institute in Eilat, Israel (Gulf of Aqaba, Red Sea) for on-site behavioral assays during the summer of 2009. Both species were easy to collect with hand-held nets that allowed minimum physical impact and rapid transfer to holding tanks. The target species were separated immediately after collection into groups of approximately 50 to 60 mixed-sex individuals and kept in 1 l jars filled with filtered seawater (FSW; 50 µm). Copepods were not fed during the 24 h prior to the behavioral assays. All experiments used FSW in the recirculating flow system under temperature and salinity conditions nearly identical to *in situ* values. All behavioral assays were run in mixed-sex, species-specific trials following a 1 h acclimation period in the apparatus. During this period the upwelling or downwelling flow was started and allowed to reach steady state while copepods were aggregated away from the flow via a point source of white light. Behavioral assays were conducted for 2 h periods for the upwelling and downwelling flow treatments (separately). Two replicates of each combination of species and treatment were performed along with two 1 h long control trials

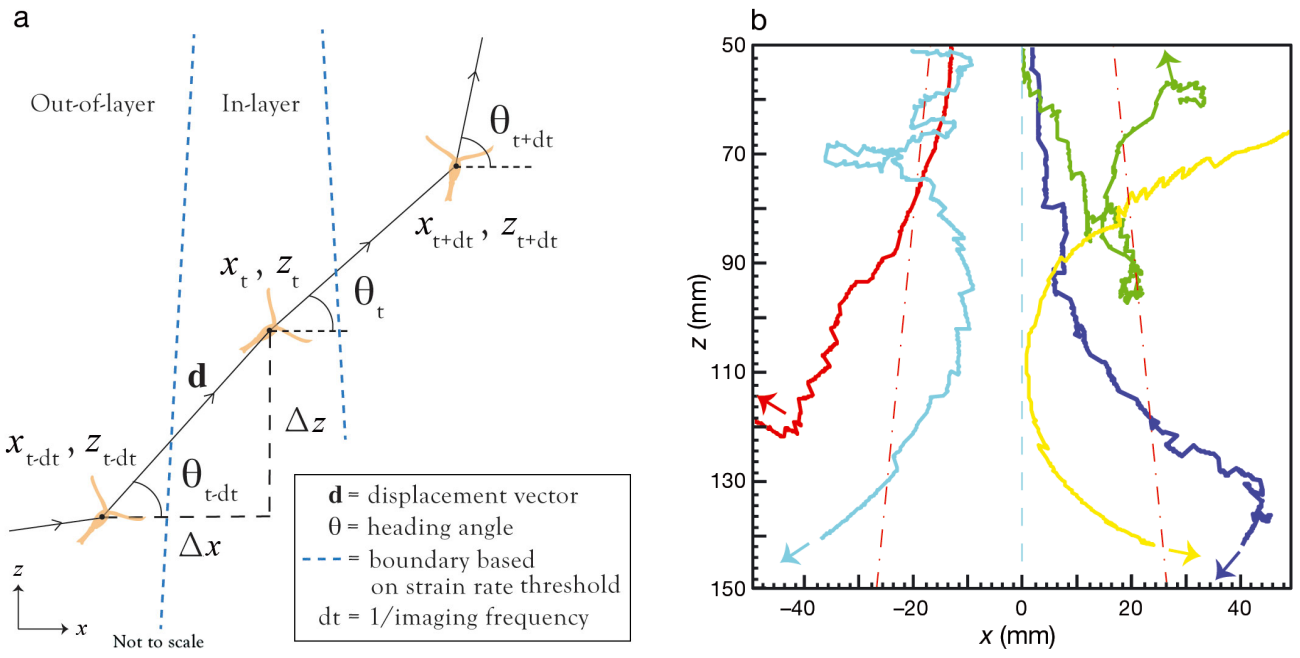

Fig. 4. (a) A hypothetical digitized trajectory defining the geometry of the displacement vector and the experimental domain, where t is time, and (b) 5 sample swimming trajectories from *Acartia negligens* in the downwelling jet; the layer boundary (red dashed line) and centerline (blue dashed line) are indicated. For definitions of *x* and *z* see Fig. 2

(i.e. no flow) for each species. Stagnant conditions were chosen as the statistical control because the jet flow velocities peaked on the centerline (middle of the observation window for the behavioral assays) and quickly decayed to stagnant conditions (~ 60% of the observation window and most of the experimental tank was effectively stagnant, Fig. 2). Thus, for statistical analyses aimed at detecting changes in behavior due to sensing velocity gradients associated with upwelling or downwelling flows in a largely stagnant experimental domain, stagnant water was a robust choice of control for statistically isolating the desired experimental treatment effects (see 'Statistical analysis' below).

Animals in all cases were filmed in a 100 × 100 mm observation window (i.e. slightly larger region than the field shown in Fig. 2a). Illumination was provided using a red diode (660 nm; Fig. 1). The test section was backlit with collimated illumination that yielded silhouettes of the swimming animals on the front surface of the test section. A sheet of film paper was placed on the front of the test section in order to increase the contrast and crispness of the silhouette. The shadowgraph trajectories were recorded via a charge-coupled device (CCD) camera (Pulnix model 745i, 768 × 494 pixels) linked to a digital video recorder (mini dv tapes). All experiments were recorded at 30 frames per second (fps), fully resolving the swimming behaviors of the tested animals.

Analysis of trajectories

The video records were digitized and individual copepod swimming trajectories were quantified using LabTrack Software (BioRAS). Fig. 4a shows a hypothetical digitized copepod trajectory in relation to relevant behavioral parameters and the in-layer and out-of-layer regions of the experimental domain, described in detail below. A sample set of trajectories for the hop-sink swimming *A. negligens* in a downwelling jet is shown in Fig. 4b. The resulting data sets, which include time and spatial (i.e. *x* and *z*) coordinate information, were post-processed in 2 phases using a suite of custom MATLAB codes.

The first phase involved determining threshold shear deformation rate values for each species that elicited significant behavioral responses. The behavior of an individual copepod was examined as the animal was exposed to varying shear deformation rates as it progressed along its trajectory (assuming no lag in response) (Woodson et al. 2005). Three specific behavioral parameters were examined as a function of shear deformation rate: relative swimming speed, turn frequency, and change in directional heading (i.e. the change in angular direction of the displacement vector with respect to the horizontal plane). For each copepod trajectory, the mean and standard deviation of each of the behavioral parameters were computed for portions of the trajectory in

regions that corresponded to being above and below the shear deformation rate value. The absolute value of the difference (i.e. difference between above and below a given shear deformation rate) was normalized by the maximum difference for the individual trajectory. The results for all trajectories were averaged. The benefit of completing analyses on individual paths and then averaging over the entire population was that it retained the variability of individual behavior while also revealing the population scale phenomena. Other hydrodynamic cues were similarly evaluated (e.g. vertical velocity magnitude), but shear deformation rate is reported here because previous studies indicated that it correlated best with behavioral responses (Fields & Yen 1997, Kiørboe & Visser 1999), it yielded the most consistent threshold results in the current analysis, and it enabled comparison with previous studies (summarized in Woodson et al. 2014). The shear deformation rate that initiated large changes in behavior indicated the threshold for which the animal perceived the layer and therefore defined the layer's spatial expanse (see 'Results').

The second phase involved computing path kinematic parameters for portions of each trajectory inside and outside the vertical flow layer (boundaries defined by the behavioral threshold level). The path kinematics computed in this study were relative swimming speed (the swimming speed of the animal minus the local fluid velocity spatially interpolated from the PIV results) and turning frequency (where a turn was defined as a change of direction of 15 degrees or more). The computed gross path characteristics included the net-to-gross displacement ratio (NGDR = net displacement/gross displacement), the vertical net-to-gross displacement ratio (VNGDR = net vertical displacement/gross vertical displacement), and the proportional vicinity time (PVT = time in observation window after contacting the layer region/total time in observation window). NGDR ranges from 0 to 1, with small values indicating curved, loopy trajectories, and values close to 1 indicating straight, direct trajectories. VNGDR can be viewed as a spectra of depth-keeping behaviors, with small values (near zero) indicating 'U-shaped'' or 'C-shaped' trajectories where active movements counteracted passive advective transport and resulted in small net vertical displacement, hence strong depth-keeping behavior. Similarly, large VNGDR values (near 1) indicated trajectories with large net vertical displacement, and thus weak depth-keeping behavior at the scale of observation. To alleviate potential dependence of NGDR and VNGDR values on trajectory duration (Tiselius 1992), the quantities were consistently computed for 4 s periods of a given trajectory and averaged.

Statistical analysis

Statistical analyses of behavioral response data were evaluated using JMP Pro 11 (2013, SAS Institute). Significance of changes in path kinematics (i.e. relative swimming speed, turn frequency) were investigated via a single factor, nested, repeated measures ANOVA between in-layer versus out-of-layer values. The single factor (or treatment) was the vertical shear flow, which has 2 treatment levels, upwelling and downwelling. The repeated measures aspect of the design indicated that in-layer versus out-of-layer values were examined and compared for each individual copepod. A general linear model (GLM) was used because of the unbalanced design, whereas the nested aspect accounted for variability across replicates (data were pooled if replicate effects were insignificant, and the pooled error variance was used). Significance of changes in gross path characteristics (PVT, NGDR, VNGDR) were evaluated via a single factor, nested ANOVA of the arcsine-transformed data sets between control and treatment (upwelling, downwelling) values; post-hoc Dunnett's control tests were used to evaluate significant differences among control, upwelling, and downwelling groups.

The repeated measures design (in-layer versus out-of-layer) was employed for the path kinematic data to better account for variability in individual copepod behaviors (e.g. males typically swim faster than females; Mauchline 1998, Woodson et al. 2005) and provides a more nuanced examination (finer spatial and shorter time scales) of changes in copepod behavior. Complimenting this design, the statistical design employed for gross path parameters (i.e. treatment vs. control) was warranted to look at behavioral changes over longer temporal and larger spatial scales and due to the fact that 1 parameter (PVT) is only defined for the entire trajectory and the others (NGDR, VNGDR) must be computed in an averaging fashion over shorter segments of a trajectory (see above section, Tiselius 1992), which renders computation of in-layer and out-of-layer values impractical.

Arcsine transformation of proportional data was warranted to comply with the ANOVA assumptions of normality and homoscedasticity (Zar 1999). For some proportional data types (binomial) the logit

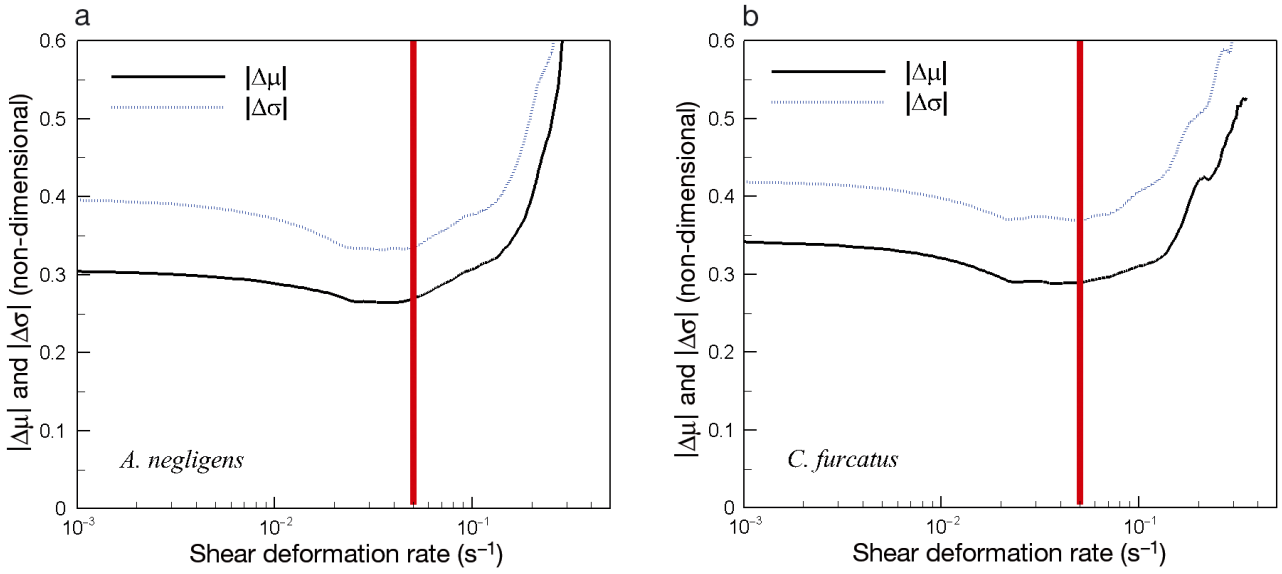

Fig. 5. Population average of the difference in the mean (Δμ) and standard deviation (Δσ) of parameters above and below the shear deformation rate value for (a) *Acartia negligens* and (b) *Clausocalanus furcatus*. For presentation clarity, the curves represent the combination of 6 differential parameters: relative swimming speed, turn frequency, and change in directional heading each in upwelling and downwelling treatments. In order to combine, the individual differential parameter curves are normalized by their maximum value to create a common range. The vertical red line indicates the selected threshold value as identified by the beginning of the rapid increase in slope of the curves

transform is superior to the arcsine transform in terms of satisfying linear modeling assumptions, statistical power, and potential for Type I statistical error (Warton & Hui 2011). For the data sets presented here, being proportional but not binomial, there is no reason to prefer one transform over the other with the potential exception of interpretability. To confirm this, the authors ran all statistical tests of proportional data sets using the logit transform and found identical significance levels everywhere. All data sets were examined and tested for normality (Shapiro-Wilk goodness-of-fit) and homoscedasticity (examination of fit-by-residual plots for fan or funnel shapes) prior to statistical analyses, revealing no significant departures.

Note that in all cases, the number of individual paths was less than the number of animals used in each experiment to minimize the possibility of repeated sampling of a given individual (pseudo-replication). This possibility was further minimized as animals tended to accumulate out of the observation window at the downstream end of the working section by the conclusion of behavioral assays. Thus, individual paths were considered as independent samples. Statistical independence was further ensured by minimizing potential copepod–copepod interactions (neighbor-induced behavioral responses) with low organism densities in the experimental domain. Previous evidence suggests that copepods need to be within 1 or 2 body lengths to influence a neighbor's swimming behavior (Yen et al. 1998). Here, approximately 60 copepods were dispersed in a 30 l volume (an average of 2 copepods in 1 l of seawater), producing an average nearest-neighbor distance of 5 to 10 cm (or roughly 25 to 50 body lengths). This renders the potential for individual interactions unlikely as reflected in the fact that more than 2 to 3 copepods were rarely observed in the observation window at any time.

RESULTS

Behavioral threshold

Significant behavioral responses, and the behavioral response threshold value, were indicated by transition in the magnitude (mean) and the variability (standard deviation) of behavior above and below a given shear deformation rate value (i.e. a visually identified rapid change in the slope of the differential curves shown in Fig. 5). The individual parameters (relative swimming speed, turn frequency, and change in directional heading) for upwelling and downwelling treatments revealed similar trends. Hence for clarity of presentation, the 6 parameters were combined for the differential of the mean and the differential of the standard deviation curves shown in

Table 1. Comparison of relative swimming speed (mm s^{-1}) for *Acartia negligens* and *Clausocalanus furcatus* in-layer and out-of-layer. The results reported in the column 'Layer-type effect' indicate the significance of behavioral differences due to the effects of an upwelling versus downwelling shear flow. The results in the column 'Location effect' indicate the significance of behavioral differences due to an individual copepod's presence in the shear layer region versus out-of-layer. The interaction results in the column 'Location × layer-type effect' indicate whether or not in-layer versus out-of-layer comparisons are contingent upon layer-type (i.e. upwelling versus downwelling). SE: standard error

Species	Treatment	n	Relative swimming speed		Layer-type effect	Location effect	Location × layer-type effect
			In-layer (SE)	Out-of-layer (SE)			
A. negligens	Upwelling	39	9.0 (0.51)	7.6 (0.36)	$F = 32.7$, $p < 0.0001$	$F = 17.5$, $p < 0.0001$	$F = 1.35$, $p = 0.25$
	Downwelling	72	6.8 (0.23)	6.0 (0.15)			
C. furcatus	Upwelling	76	6.6 (0.31)	5.2 (0.30)	$F = 2.1$, $p = 0.15$	$F = 6.4$, $p = 0.013$	$F = 6.2$, $p = 0.015$
	Downwelling	40	6.5 (0.42)	6.6 (0.54)			

Table 2. Comparison of turn frequency (turns $ind.^{-1}$ s^{-1}) for *Acartia negligens* and *Clausocalanus furcatus* in-layer and out-of-layer. The results reported in the column 'Layer-type effect' indicate the significance of behavioral differences due to the effects of an upwelling versus downwelling shear flow. The results in the column 'Location effect' indicate the significance of behavioral differences due to an individual copepod's presence in the shear layer region versus out-of-layer. The interaction results in the column 'Location × layer-type effect' indicate whether or not in-layer versus out-of-layer comparisons are contingent upon layer-type (i.e. upwelling versus downwelling). SE: standard error

Species	Treatment	n	Turn frequency		Layer-type effect	Location effect	Location × layer-type effect
			In-layer (SE)	Out-of-layer (SE)			
A. negligens	Upwelling	39	6.7 (0.35)	7.0 (0.24)	$F = 7.0$, $p = 0.009$	$F = 0.6$, $p = 0.43$	$F = 4.5$, $p = 0.035$
	Downwelling	72	6.5 (0.17)	5.9 (0.19)			
C. furcatus	Upwelling	76	6.1 (0.20)	5.8 (0.17)	$F = 1.1$, $p = 0.29$	$F = 4.3$, $p = 0.04$	$F = 0.1$, $p = 0.73$
	Downwelling	40	5.9 (0.26)	5.4 (0.35)			

Fig. 5. The combined behavioral response curve revealed a change in slope at around 0.05 s^{-1}, which was representative of the threshold transition for both species (vertical red line in Fig. 5). The selected behavioral deformation rate threshold of 0.05 s^{-1} marks the transition to a behaviorally relevant range of deformation rates that elicited significant responses as indicated by the positive rate of change of the slope of the threshold curve with increasing shear deformation rate values.

In-layer versus out-of-layer behavior

Acartia negligens

Acartia negligens increased relative swimming speed in-layer versus out-of-layer (location effect, $p < 0.0001$; Table 1) and also increased swimming speeds in the upwelling and downwelling flows (layer-type effect, $p < 0.0001$; Table 1). Upwelling and downwelling flows produced similar responses (location × layer-type effect, $p = 0.25$; Table 1).

Although there was a layer-type effect on turn frequency ($p = 0.009$; Table 2), it appeared to be due to the increase in turn frequency when *A. negligens* was presented with a downwelling flow. Upwelling flows showed very similar turn frequencies in-layer versus out-of-layer, with a significant interaction term ($p = 0.035$; Table 2) that likely obscured the significance of individual levels of the main effect (i.e. location effects for upwelling and downwelling conditions, $p = 0.43$; Table 2).

Both upwelling and downwelling flows produced significant increases in PVT (i.e. more time spent in or near the layer region) when compared to control values ($p < 0.0001$; Table 3). Both upwelling and downwelling flows also produced significant increases in NGDR (i.e. straighter trajectories) ($p < 0.0001$; Table 3) and in VNGDR ($p < 0.0001$; Table 3) when compared to control values. Coupled with increased relative swimming speeds, the presence of the vertical shear flows induced vertical transport with high net vertical displacement.

For *A. negligens*, it was clear that even though the average value of VNGDR increased, there was con-

Table 3. Comparison of proportional vicinity time (PVT), net-to-gross-displacement ratio (NGDR), and vertical-net-to-gross-displacement ratio (VNGDR) for *Acartia negligens* and *Clausocalanus furcatus*. *F*-values are for all treatments for each species

Species	Treatment	n	PVT (SE)	*F*	p	NGDR (SE)	*F*	p	VNGDR (SE)	*F*	p
A. negligens	Control	54	0.63 (0.06)	9.8	–	0.34 (0.01)	45.9	–	0.37 (0.02)	36.8	–
	Upwelling	39	0.92 (0.04)		<0.0001	0.69 (0.03)		<0.0001	0.78 (0.03)		<0.0001
	Downwelling	72	0.87 (0.03)		<0.0001	0.57 (0.02)		<0.0001	0.65 (0.03)		<0.0001
C. furcatus	Control	24	0.51 (0.09)	8.3	–	0.34 (0.03)	13.4	–	0.33 (0.04)	12.5	–
	Upwelling	76	0.80 (0.04)		<0.0001	0.64 (0.02)		<0.0001	0.70 (0.02)		<0.0001
	Downwelling	40	0.86 (0.04)		<0.0001	0.62 (0.03)		<0.0001	0.69 (0.04)		<0.0001

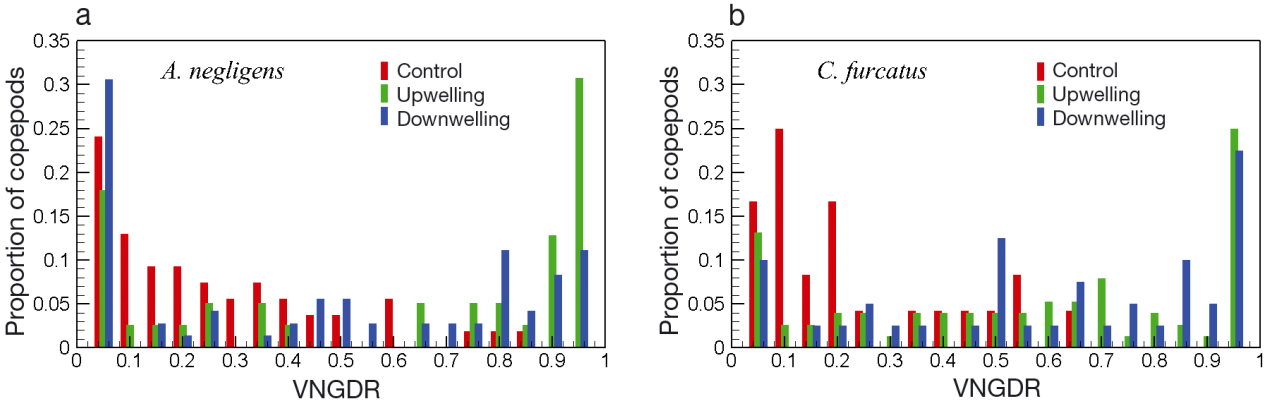

Fig. 6. Vertical net-to-gross displacement ratios (VNGDR) for control (stagnant fluid) and upwelling and downwelling treatments for (a) *Acartia negligens* and (b) *Clausocalanus furcatus*. The bimodality of the treatment histograms indicated that a portion of the population exhibited large net vertical transport and another portion exhibited depth-keeping behavior at the scale of observation

siderable spread with high frequencies of both small and large values resulting in a bimodal distribution (Fig. 6a). This suggested that different portions of the population were explicitly exhibiting depth-keeping behavior (small VNGDR) and large net vertical transport (large VNGDR). For portions of the population exhibiting large net vertical transport with little to no explicit depth-keeping behavior at the scale of the observation (i.e. VNGDR > 0.75), the time spent swimming with the flow versus against the flow revealed that *A. negligens* spent a considerable amount of time attempting to resist vertical advection by swimming against the flow (Fig. 7; ~45% in upwelling treatment, ~90% in downwelling treatment).

Clausocalanus furcatus

In the presence of vertical shear flows, *Clausocalanus furcatus* significantly changed relative swimming speeds in-layer versus out-of-layer (location effect, p = 0.013; Table 1). However, responses to upwelling and downwelling flows were significantly different (location × layer-type effect, p = 0.015; Table 1), with relative swimming speeds increasing

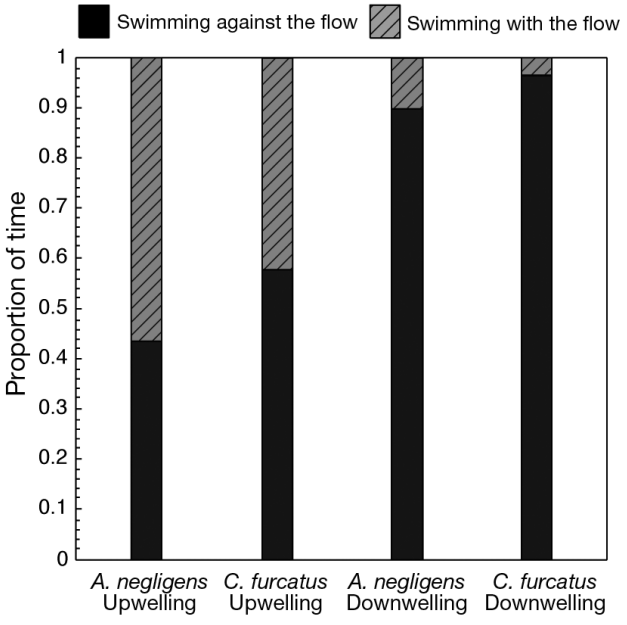

Fig. 7. Proportion of time spent swimming with and against the flow for *Acartia negligens* and *Clausocalanus furcatus* exhibiting vertical net-to-gross displacement ratio (VNGDR) > 0.75 (i.e. little to no explicit depth-keeping at the scale of the trajectory observation)

for upwelling conditions and remaining statistically unchanged for downwelling conditions (Table 1). The location × layer-type interaction likely obscured any effect of the layer-type itself; relative swimming speeds were, on average, not significantly different for upwelling and downwelling flows (layer-type effect, $p = 0.15$; Table 1). *C. furcatus* showed significant increases in turn frequency in-layer versus out-of-layer for both upwelling and downwelling flows (location effect, $p = 0.04$; location × layer-type effect, $p = 0.73$; Table 2), and there was no effect of the layer-type ($p = 0.29$; Table 2).

C. furcatus increased PVT in both upwelling and downwelling flows when compared to control values ($p < 0.0001$; Table 3). Thus, the presence of horizontal gradients of vertical velocity alone appeared sufficient to cause fine-scale, population-level aggregations of *C. furcatus*. NGDR increased significantly for both upwelling and downwelling flows when compared to control values ($p < 0.0001$; Table 3), indicating that copepod trajectories became more linear and less sinuous (consistent with *A. negligens*) in the presence of the vertical shear layer. Finally, VNGDR also increased significantly for both upwelling and downwelling flows when compared to control values ($p < 0.0001$; Table 3), which indicated large net vertical transport.

Examining the distribution of VNGDR (Fig. 6b) again highlighted response variability that was obscured by the population level trends. Even though the average value of VNGDR increased, VNGDR showed strong peaks in both large values (high net vertical displacement) and small values (low net vertical displacement). This resulted in a bimodal distribution and suggested that significant portions of the population were explicitly exhibiting both depth-keeping behavior (small VNGDR values) and large net vertical transport (large VNGDR values). The sub-population of *C. furcatus* that exhibited large net vertical transport with little to no explicit depth-keeping behavior at the scale of the observation (i.e. VNGDR > 0.75) spent a considerable amount of time attempting to resist vertical advection by swimming against the flow (Fig. 7; ~55% in upwelling treatment, ~95% in downwelling treatment).

In summary, both *A. negligens* and *C. furcatus* responded to upwelling and downwelling shear flows with increases in relative swimming speed and turning frequency (Tables 1 & 2). Although upwelling versus downwelling flows sometimes elicited different responses for a particular species–behavior combination, the most common pattern was for animals to swim faster and turn more frequently when exposed to the layer. Moreover, the end result of these behavioral changes was that animals spent more time in and near the layer region and showed greater vertical displacement on average, irrespective of the flow direction (Table 3). Despite this, a substantial proportion of individuals in both species exhibited depth-keeping behavior in both upwelling and downwelling flows (Fig. 6). For the proportion of individuals of both species exhibiting high VNGDR (i.e. little to no explicit depth-keeping behavior at the scale of the observation), a considerable amount of time was spent in swimming against the flow in an attempt to resist vertical advection (Fig. 7).

DISCUSSION

Both species demonstrated a clear behavioral response to the flow structure (i.e. flow aligned in the vertical direction with horizontal gradients). Despite some variation in the response of the kinematic parameters, gross path characteristics (PVT, NGDR, and VNGDR) all increased relative to control values in both species and in both flow types (i.e. laboratory mimic of upwelling and downwelling fronts). The shear deformation rate threshold value for response (0.05 s^{-1} for both species) was comparable to those previously reported for *Acartia tonsa* (0.035 to 0.06 s^{-1}) and *Temora longicornis* (0.03 to 0.06 s^{-1}) for horizontal shear layers (i.e. flow aligned in the horizontal direction with vertical gradients; Woodson et al. 2005). For both clines (vertical gradients, horizontally aligned flow) and fronts (horizontal gradients, vertically aligned flow), the threshold shear deformation rate for behavioral response to the environmental flow structure was substantially smaller than that for escape response, which was 1 to 2 orders of magnitude greater, depending on species (tabulated in Woodson et al. 2014).

Upwelling versus downwelling

Our data suggested that the presence of horizontal gradients of vertical velocity was an important sensory cue and that the direction of vertical flow was largely unimportant in the absence of other sensory cues. This was indicated by the similarity of behavioral responses to upwelling and downwelling shear layers for each species and the manner in which changes in path kinematic parameters affected gross path characteristics and trajectory shape (i.e. PVT, NGDR, VNGDR; Table 3). The effect of vertical shear

flows on fine-scale copepod behavior, regardless of flow direction, was always an attractive cue, rather than an aversive or dispersive stimulus. Additionally, shear-induced changes in VNGDR histograms for each species indicated that portions of each population were exhibiting explicit depth-keeping behavior via 'U-' or 'C-shaped' trajectories for both upwelling and downwelling flows. Conversely, individuals of both species that exhibited large net vertical transport with little to no depth-keeping behavior at the scale of the observation were spending a high percentage of time attempting to swim against the flow, particularly in the downwelling treatment (roughly twice as much time compared to the upwelling treatment; Fig. 7), which indicated an active resistance to vertical advection. This is consistent with the field observation that zooplankton maintain depth by 'swimming against the flow' and produce patchy distributions (Genin et al. 2005). Therefore, as an aggregative cue that often induces depth-keeping behavior, a persistent vertical shear layer likely acts to generate patchiness in coastal marine ecosystems on a variety of spatio-temporal scales.

Acartia negligens versus *Clausocalanus furcatus*

Overall, the hop-sink swimming *A. negligens* and the cruise-swimming *C. furcatus* each responded similarly to upwelling and downwelling shear flows in terms of path kinematic parameters (relative swimming speed and turn frequency) (Tables 1 & 2). For both species, relative swimming speed in-layer was greater than out-of-layer, with the exception of *C. furcatus* in the downwelling layer, in which speed remained statistically unchanged (Table 1). This indicated that copepods typically were maintaining greater swimming speeds than ambient vertical flow velocities, a necessary precursor to depth-keeping behavior. Similarly, for both copepods, turn frequency in-layer was always greater than out-of-layer, with the exception of *A. negligens* in the upwelling layer, in which turn frequency remained unchanged (Table 2). Thus, in the absence of other sensory cues, copepod behavioral responses to both upwelling and downwelling shear flows were predominantly excited behaviors. Increasing relative swimming speed and turn frequency in response to shear flow structure allows copepods to effectively sample the surrounding volume and use the available hydrodynamic information to make decisions that optimize habitat partitioning and life success (Woodson et al. 2005, 2007a,b).

Patchiness and depth maintenance

Sensory cues, such as light, salinity, temperature, fluid density, and chemicals are known to produce copepod aggregations in and near environmental structure (e.g. Woodson et al. 2014). Here, the results indicated that fluid motion and hydrodynamic cues produce behavioral responses that generate patchy population distributions. Convincing evidence for individual and population-level patchiness and depth-keeping behavior was revealed by changes in path kinematics, gross path characteristics, and histograms. Our data explicitly revealed that vertical shear flows caused trajectories to become excited (typically increased relative swimming speed and turning frequency in-layer) and more ballistic (increased NGDR values) in both species. Excited in-layer behaviors and fundamental changes to trajectory characteristics indicated that upwelling and downwelling fronts could act as physical boundaries of ecological significance leading to horizontally patchy distributions given persistent hydrodynamic features (as explicitly seen in the increased PVT values). In the fringe reef system where the copepods were collected, zooplankton distributions are consistently affected by the upwelling and downwelling fronts due to depth retention by many zooplankters (Genin et al. 2005).

For *A. negligens* and *C. furcatus*, even though VNGDR increased on average (Table 3), there was also a preferential spread of VNGDR values towards both small and large values resulting in a bimodal distribution (Fig. 6). This suggested that a substantial portion of the population was exhibiting depth-keeping behavior (small VNGDR values) while another portion exhibited large net vertical transport (large VNGDR values) even while investing a considerable amount of time swimming against the flow, attempting to resist vertical advection (Fig. 7). Thus, copepods may resist large-scale vertical advection through depth-keeping behavior when gradients of vertical velocity are coherent and sensible and other sensory cues are absent, likely leading to vertically patchy distributions. Individual copepods resisting large-scale net vertical advection can produce population-level aggregations within a finite region of the water column (as optimized by reduced predation risk and prey/mate availability).

Acknowledgements. Financial support was provided by US National Science Foundation grant OCE-0728238 to D.R.W., M.J.W. and J.Y. and by an Israel Science Foundation grant to A.G. We thank Margarita Zarubin and Viviana Bracha Farstey for assistance with the collection and identification of copepods.

LITERATURE CITED

Cornils A, Schnack-Schiel SB, Al-Najjar T, Badran MI, Rasheed M, Manasreh R, Richter C (2007a) The seasonal cycle of the epipelagic mesozooplankton in the northern Gulf of Aqaba (Red Sea). J Mar Syst 68:278–292

Cornils A, Schnack-Schiel SB, Böer M, Graeve M, Struck U, Al-Najjar T, Richter C (2007b) Feeding of clausocalanids (Calanoida, Copepoda) on naturally occurring particles in the northern Gulf of Aqaba (Red Sea). Mar Biol 151: 1261–1274

Dasi LP, Schuerg F, Webster DR (2007) The geometric properties of high-Schmidt-number passive scalar iso-surfaces in turbulent boundary layers. J Fluid Mech 588: 253–277

Dubischar CD, Lopes RM, Bathmann UV (2002) High summer abundances of small pelagic copepods at the Antarctic Polar Front — implications for ecosystem dynamics. Deep-Sea Res II 49:3871–3887

Fields DM, Yen J (1997) The escape behavior of marine copepods in response to a quantifiable fluid mechanical disturbance. J Plankton Res 19:1289–1304

Folt CL, Burns CW (1999) Biological drivers of zooplankton patchiness. Trends Ecol Evol 14:300–305

Franks PJS (1992) Sink or swim: accumulation of biomass at fronts. Mar Ecol Prog Ser 82:1–12

Genin A (2004) Bio-physical coupling in the formation of zooplankton and fish aggregations over abrupt topographies. J Mar Syst 50:3–20

Genin A, Jaffe JS, Reef R, Richter C, Franks PJS (2005) Swimming against the flow: a mechanism of zooplankton aggregation. Science 308:860–862

Greer AT, Cowen RK, Guigand CM, Hare JA (2015) Fine-scale planktonic habitat partitioning at the shelf-slope front revealed by high-resolution imaging system. J Mar Syst 142:111–125

Herman AW, Sameoto DD, Longhurst AR (1981) Vertical and horizontal distribution patterns of copepods near the shelf break south of Nova Scotia. Can J Fish Aquat Sci 38:1065–1076

Kiørboe T, Visser AW (1999) Predator and prey perception in copepods due to hydromechanical signals. Mar Ecol Prog Ser 179:81–95

Labiosa RG, Arrigo KR, Genin A, Monismith SG, van Dijken G (2003) The interplay between upwelling and deep convective mixing in determining the seasonal phytoplankton dynamics in the Gulf of Aqaba: evidence from SeaWiFS and MODIS. Limnol Oceanogr 48:2355–2368

Landry MR, Ohman MD, Goericke R, Stukel MR, Barbeau KA, Bundy R, Kahru M (2012) Pelagic community responses to a deep-water front in the California current ecosystem: overview of the A-Front study. J Plankton Res 34:739–748

Largier JL (1993) Estuarine fronts: How important are they? Estuaries 16:1–11

Lennert-Cody CE, Franks PJS (1999) Plankton patchiness in high-frequency internal waves. Mar Ecol Prog Ser 186: 59–66

Manasrah R, Badran M, Lass HU, Fennel WG (2004) Circulation and winter deep-water formation in the northern Red Sea. Oceanologia 46:5–23

Mann KH, Lazier JRN (2006) Dynamics of marine ecosystems: Biological-physical interactions in the oceans. Blackwell Science, Malden, MA

Mauchline J (1998) The biology of calanoid copepods. Elsevier Academic Press, San Diego, CA

Mazzocchi MG, Paffenhöfer GA (1998) First observations on the biology of *Clausocalanus furcatus* (Copepoda, Calanoida). J Plankton Res 20:331–342

Mazzocchi MG, Paffenhöfer GA (1999) Swimming and feeding behaviour of the planktonic copepod *Clausocalanus furcatus*. J Plankton Res 21:1501–1518

McClatchie S, Cowen R, Nieto K, Greer A and others (2012) Resolution of fine biological structure including small narcomedusae across a front in the Southern California Bight. J Geophys Res Oceans 117:C04020, doi: 10.1029/2011JC007565

McManus MA, Woodson CB (2012) Plankton distribution and ocean dispersal. J Exp Biol 215:1008–1016

Munk P (2014) Fish larvae at fronts: Horizontal and vertical distributions of gadoid fish larvae across a frontal zone at the Norwegian Trench. Deep-Sea Res II 107:3–14

Peralba A, Mazzocchi MG (2004) Vertical and seasonal distribution of eight Clausocalanus species (Copepoda: Calanoida) in oligotrophic waters. ICES J Mar Sci 61: 645–653

Prado-Por MSD (1983) The diversity and dynamics of Calanoida (Copepoda) in the northern Gulf of Elat (Aqaba), Red Sea. Oceanol Acta 6:139–145

Raffel M, Willert C, Kompenhans J (1998) Particle image velocimetry: a practical guide. Springer-Verlag, Berlin

Tiselius P (1992) Behavior of *Acartia tonsa* in patchy food environments. Limnol Oceanogr 37:1640–1651

True AC (2011) Patchiness: Zooplankton behavior in fine-scale vertical shear layers. MS thesis, Georgia Institute of Technology, Atlanta, GA

Uttieri M, Paffenhöfer GA, Mazzocchi MG (2008) Prey capture in *Clausocalanus furcatus* (Copepoda: Calanoida). The role of swimming behaviour. Mar Biol 153:925–935

Warton DI, Hui FKC (2011) The arcsine is asinine: the analysis of proportions in ecology. Ecology 92:3–10

Wolanski E, Hamner WM (1988) Topographically controlled fronts in the ocean and their biological influence. Science 241:177–181

Woodson CB, Webster DR, Weissburg MJ, Yen J (2005) Response of copepods to physical gradients associated with structure in the ocean. Limnol Oceanogr 50: 1552–1564

Woodson CB, Webster DR, Weissburg MJ, Yen J (2007a) Cue hierarchy and foraging in calanoid copepods: ecological implications of oceanographic structure. Mar Ecol Prog Ser 330:163–177

Woodson CB, Webster DR, Weissburg MJ, Yen J (2007b) The prevalence and implications of copepod behavioral responses to oceanographic structure. Integr Comp Biol 47:831–846

Woodson CB, Webster DR, True AC (2014) Copepod behavior: oceanographic cues, distributions, and trophic interactions. In: Seuront L (ed) Copepods: diversity, habitat and behavior. Nova Science Publishers, New York, NY, p 215–253

Yen J, Weissburg MJ, Doall MH (1998) The fluid physics of signal perception by mate-tracking copepods. Philos Trans R Soc Lond B Biol Sci 353:787–804

Zar JH (1999) Biostatistical analysis, 4th edn. Prentice Hall, Upper Saddle, NJ

Editorial responsibility: Alejandro Gallego, Aberdeen, UK

Submitted: May 21, 2015; Accepted: September 2, 2015
Proofs received from author(s): November 2, 2015